

Multiple reversals of vortex ratchet effects in a superconducting strip with inclined dynamic pinning landscape

An He(何安) and Cun Xue(薛存)

Citation: Chin. Phys. B, 2020, 29 (**12**): 127401. DOI: 10.1088/1674-1056/abbb

Journal homepage: http://cpb.iphy.ac.cn; http://iopscience.iop.org/cpb

What follows is a list of articles you may be interested in

Phase-field simulation of superconductor vortex clustering in the vicinity of ferromagnetic domain bifurcations

Hasnain Mehdi Jafri, Jing Wang(王静), Chao Yang(杨超), Jun-Sheng Wang(王俊升), and Hou-Bing Huang(黄厚兵)
Chin. Phys. B, 2020, 29 (**12**): 127402. DOI: 10.1088/1674-1056/abb22c

Anisotropy of $Ca_{0.73}La_{0.27}(Fe_{0.96}Co_{0.04})As_2$ studied by torque magnetometry

Ya-Lei Huang(黄亚磊), Run Yang(杨润), Pei-Gang Li(李培刚), Hong Xiao(肖宏)
Chin. Phys. B, 2020, 29 (**9**): 097405. DOI: 10.1088/1674-1056/ab9f26

Topological superconductivity in a $Bi_2Te_3/NbSe_2$ heterostructure: A review

Hao Zheng(郑浩), Jin-Feng Jia(贾金锋)
Chin. Phys. B, 2019, 28 (**6**): 067403. DOI: 10.1088/1674-1056/28/6/067403

Superconductivity in self-flux-synthesized single crystalline $R_2Pt_3Ge_5$(R = La, Ce, Pr)

Q Sheng(盛琪), J Zhang(张建), K Huang(黄百畅), Z Ding(丁兆峰), X Peng(彭小冉), C Tan(谭程), L Shu(殳蕾)
Chin. Phys. B, 2017, 26 (**5**): 057401. DOI: 10.1088/1674-1056/26/5/057401

Critical current density behaviors across a grain boundary inclined to current with different angles in $YBa_2Cu_3O_{7-\delta}$ bicrystal junctions

Tao Hua(花涛), Wei-Wei Xu(许伟伟), Zheng-Ming Ji(吉争鸣), Da-Yuan Guo(郭大元), Qing-Yun Wang(王青云), Xiang-Rong Ma(马湘蓉), Rui-Yu Liang(梁瑞宇)
Chin. Phys. B, 2016, 25 (**6**): 067401. DOI: 10.1088/1674-1056/25/6/067401

Multiple reversals of vortex ratchet effects in a superconducting strip with inclined dynamic pinning landscape*

An He(何安)[1,2] and Cun Xue(薛存)[3,†]

[1] College of Science, Chang'an University, Xi'an 710064, China
[2] School of Aeronautics, Northwestern Polytechnical University, Xi'an 710072, China
[3] School of Mechanics, Civil Engineering and Architecture, Northwestern Polytechnical University, Xi'an 710072, China

(Received 4 May 2020; revised manuscript received 11 September 2020; accepted manuscript online 28 September 2020)

Using time-dependent Ginzburg–Landau formalism, we investigate the multiple reversals of ratchet effects in an unpatterned superconducting strip by the tilted dynamic pinning potential. In the case of collinear sliding potential and Lorentz force, vortices are always confined in the channels induced by sliding potential. However, due to the inclination angle of sliding pinning potential with respect to the Lorentz force, vortices could be driven out of the channels, and unexpected results with multiple reversals of vortex rectifications are observed. The mechanism of multiple reversals of vortex rectifications is explored by analyzing different vortex motion scenarios with increasing ac current amplitudes. The multiple reversals of transverse and longitudinal ratchet effects can be highly controlled by ac amplitude and dynamic pinning velocity. What's more, at certain large current the ratchet effect reaches strongest within a wide range of pinning sliding velocity.

Keywords: multiple reversal, ratchet effect, dynamic pinning potential, Lorentz force

PACS: 74.25.Ha, 74.25.–q, 74.25.Wx, 74.78.Fk **DOI:** 10.1088/1674-1056/abbbe5

1. Introduction

The guidance of vortices by artificial defects such as special arrangements of antidots and magnetic nanostructures is important for general understanding of vortex matter and application of superconductors. It should be noted that the first basic explanation of the angular dependence of the guidance vortices via rows of antidots is given by the *n*-channel model.[1,2] It was pointed out that the component parallel to the applied current contributes to the Hall voltage signal. Magnetic force microscopy (MFM) has been used to manipulation and image the individual vortices in a detwinned YBCO single crystal.[3] Moreover, it was numerically reported that the MFM tip as an individual trap allows multiple superconducting vortices to move at the same time in periodic pinning arrays.[4]

Recently, in order to drag superconducting vortices, one can use dynamic pinning array with different inclination angles to provide the possibility of inducing longitudinal and Hall voltage in the absence of applied current. What will happen in a current-carrying superconductor? We know that vortex rectifications occur as drifting vortices along an "easy" direction when asymmetric potential is introduced to break the inversion symmetry for the vortex motion. Lee *et al.* first proposed to use the ratchet effect to remove the unwanted magnetic flux trapped in superconducting devices.[5]

Moreover, the reversibility in vortex ratchet systems has attracted tremendous interests so far. Villegas *et al.*[6] observed the reversal of vortex ratchet effect due to the interaction between the vortices trapped on the magnetic nanostructures and the interstitial vortices. Subsequently, the multiple reversal of ratchet effect was controlled by increasing vortex density in an array of nanometre-scale asymmetric traps,[7,8] by different periods of the asymmetric pinning potential[9–13] or conformal pinning arrays,[14] etc. The asymmetric sample geometries[15,16] were also introduced to explore the vortex ratchet effect, such as the corner-shaped superconducting microstrips[15] and strips with indentations on one lateral edge.[17]

Additionally, the ratchet effect without spatial asymmetry was investigated by varying time-asymmetric oscillations of the drive.[18] Compared to the mostly static asymmetric pinning sites used in superconductors, Wang *et al.*[19] proposed to tune the vortex ratchet effect by reprogramming the vortex ratchet potential using different spin-ice states of a magnetic overlayer. The stroboscopic effect and velocimetry[20,21] were studied by dynamic pinning landscape. Recently, the switchable vortex ratchet effect with dynamic pinning potential is reported.[22] Due to the collinear Lorentz force and sliding pinning potential, there is no Hall voltage. In the present work, we propose an asymmetric dynamic pinning landscape by a tilted sliding pinning potential in an unpatterned superconducting strip as illustrated in Section 2. The vortex dynamics and

*Project supported by the National Natural Science Foundation of China (Grant Nos. 11702034, 11972298, and 11702218), the China Postdoctoral Science Foundation (Grant No. 2019M663812), the Fundamental Research Funds for the Central Universities, China (Grant Nos. 300102129104, 3102018zy013, and 3102017jc01003), and the Young Talent Fund of University Association for Science and Technology in Shaanxi, China (Grant Nos. 20180503 and 20180501).

†Corresponding author. E-mail: xuecun@nwpu.edu.cn

© 2020 Chinese Physical Society and IOP Publishing Ltd

ratchet effects are studied by the time-dependent Ginzburg–Landau theory. We find the multiple reversals of rectification and anomalous Hall voltage oscillation in Section 3. Finally, the conclusions are given in Section 4.

2. Model system and theoretical approach

For the model system, as shown in Fig. 1, we consider a thin unpatterned superconducting film in width w and infinite length along the x axis. The sample is exposed to a perpendicular magnetic field H_a. The sliding potential can be created by means of sliding mask which keeps moving at an angle of $\theta = 45^\circ$ with respect to the x axis (the angle is -135° opposite to the sliding potential). The irradiation source goes through the sliding mask. This can lead to hot spots in the superconducting film. Thus the array of dynamic pinning potential appears and also moves across the sample at $\theta = 45^\circ$. The driving potential landscape can stem from, e.g., a famous Giaever dc transformer device,[24–27] an array of magnetic dots,[28,29] dynamic spatially periodic light excitation,[23] shifting traps as those were successfully used to manipulate colloidal particles,[30–34] or inhomogeneous magnetic field.[35] Here the tilted array of circular pinning sites of radius $R = 120$ nm with sliding velocity v_p is presented. The periods are $d_1 = 800$ nm $d_2 = 377$ nm in the parallelogram lattice, respectively.

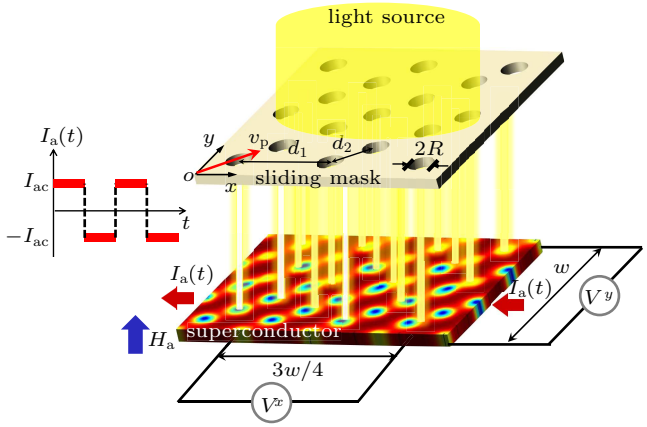


Fig. 1. Schematic diagram of the studied system with dynamic pinning potential inclined at 45° with respect to the x axis. Layouts of a sliding mask for square lattice with radius R and distance interval d. An unpatterned superconducting film of width W is applied by a square-wave ac current $I_a(t)$ and a perpendicular magnetic field H_a. The longitudinal voltage V^x and transverse voltage V^y are measured parallel and perpendicular to the direction of applied current, respectively.

In order to explore the vortex ratchet effect in such a system, a square-wave ac current $I_a(t)$ is applied to the thin (thickness $d \ll \xi, \lambda$) superconductor along the x axis. The sliding potential could promote or suppress the vortex motion for $+I_a$ and $-I_a$ depending on the applied currents. This can break the inversion symmetry of vortex motion. We perform numerical simulations based on the generalized time-dependent Ginzburg–Landau (tdGL) equations in the gauge of zero electric potential as follows:[20,36,37]

$$\frac{u}{\sqrt{1+\gamma^2|\psi|^2}}\left(\frac{\partial}{\partial t}+\frac{\gamma^2}{2}\frac{\partial|\psi|^2}{\partial t}\right)\psi = (\nabla - \mathrm{i}\boldsymbol{A})^2\psi + \left(f(t,\boldsymbol{r}) - |\psi|^2\right)\psi, \quad (1)$$

$$\frac{\partial \boldsymbol{A}}{\partial t} = \mathrm{Re}\left[\psi^*(-\mathrm{i}\nabla - \boldsymbol{A})\psi\right] - \kappa^2\nabla\times\nabla\times\boldsymbol{A}. \quad (2)$$

Here, the distances are scaled by the coherence length ξ at the working temperature, the order parameter ψ by its equilibrium value in the absence of applied current and magnetic field, the vector potential $\boldsymbol{A}$ by $\Phi_0/2\pi\xi(T)$, the time by the Ginzburg–Landau relaxation time, $\tau_{GL} = \pi\hbar/8k_B(T_c - T)u$ and the magnetic field H_a by $H_{c2} = \Phi_0/2\pi\xi^2$. The current density is in units of $j_0 = \sigma_n\hbar/2e\tau_{GL}\xi$.

The voltages V^x and V^y, in units of $\varphi_0 = \hbar/2e\tau_{GL}$, can be calculated by $\int \partial\boldsymbol{A}/\partial t\,\mathrm{d}\boldsymbol{l}$ between two points separated by a distance $3w/4$ along x direction and w along y direction, respectively. Accordingly, V_{dc} is the net dc voltage within one period of a square-wave ac current. In this study, the longitudinal ratchet effect measured along the direction of applied current is denoted by V^x_{dc}. In addition, the transverse dc voltage denoted by V^y_{dc} can also be observed, which is perpendicular to the direction of applied current. The parameter $u = 5.79$ is a suitable value for most low-T_c superconductors according to the microscopic theory.[36,38] Parameter γ accounts for inelastic scattering (dirtiness) of the superconducting film, and we take a reasonable value $\gamma = 20$ for all simulations in the main text.[39,40]

The function $f(t,\boldsymbol{r})$ describes the dynamic pinning potential in the superconducting strip. Such a pinning potential is the suppression of order parameter by local heating up to critical temperature T_c in the depletion region (see detail in Ref. [20]). It is known that $f = 0$ (or 1) in the perturbed (unperturbed) regions of the sample. The infinite sample along the x directions is implemented through periodic boundaries conditions, i.e., $\psi(x,y) = \psi(x+L,y)$ and $\boldsymbol{A}(x,y) = \boldsymbol{A}(x+L,y)$, where $L = 3w/4$ is the length of the simulated part of the strip. The superconductor-vacuum boundary condition $(\nabla - \mathrm{i}\boldsymbol{A})\psi|_n = 0$ is used at all sample edges. The applied current is introduced via the boundary condition for the vector potential $\nabla\times\boldsymbol{A}|_z(y=0,w) = H_a \pm H_I$, where $H_I = 2\pi I_a/c$ is the magnetic field induced by the current I_a.[40] In the following, $\xi = 73.8$ nm, $\kappa = 4$, $w = 2.4$ μm in our simulations are adopted, which are representatives of thin film superconductors in the literature. For comparison, typical Nb thin films have $\xi(0) = 10$ nm and $\kappa = 15$,[41] for Al films it has been reported that $\xi(0) = 90$ nm and $\kappa \sim 2$ before,[42] whereas for Pb, $\xi(0) = 34$ nm and $\kappa \sim 2$.[43] Since the effective penetration depth is dependent on thickness of the superconducting film, it can be varied in a large range of values without significantly altering T_c or ξ. In other words, the chosen values for

the parameters used in our simulations are somewhat closer to those reported for Al films.

3. Results and discussion

Let us first discuss the evolution of the rectified dc voltage with ac current amplitude at magnetic field $H_a = 0.1$. Figures 2(a) and 2(b) show the rectified voltages V_{dc}^x and V_{dc}^y, i.e., dc voltage within one cycle of applied ac current measured along x direction and y direction, respectively. Additionally, the voltages V^x and V^y represent the average values only for positive applied current $+I_a$ and only for the negative applied current $-I_a$ measured along x and y directions, respectively (see Figs. 2(c) and 2(d)). Here we use the absolute values of V^x and V^y both for $+I_a$ and $-I_a$ in order to compare with the difference between the voltages in the cases of $+I_a$ and $-I_a$. It can be found that there are four regions with several sign variations of rectified voltage by increasing ac current amplitude. Although the reversal mechanism of vortex rectifications was revealed by the change of "easy direction" of vortex motion in the channels induced by sliding potential,[22] it is definitely insufficient to understand such unexpected results with multiple reversals of vortex rectifications observed here. Compared with our previous work, we can definitely attribute it to the sliding direction of the dynamic pinning potential with respect to the Lorentz force. Therefore, in the following text, we try to explore the origin of multiple reversals of vortex rectifications in different regions by analyzing the vortex motions obtained with the powerful TDGL simulations. By considering that one should not put all analyses on the basis of powerful but "non-obvious" TDGL simulations, of course, we also try to present a simple way to capture the underlying physics.

One can see a positive rectified voltage V_{dc}^x in region I, which is small especially at small currents. As shown in Fig. 2(e), on the one hand, due to the suppression of superconductivity in the sliding channels by the dynamic pinning potential, both 45° and −135° are easier directions than other degree directions. Although the Lorentz force F_L is not parallel to the sliding channel, F_L is not sufficient to drive the vortices out of their easy directions (i.e., sliding channels). On the other hand, the vortices along 45° are slower than v_p for $+I_a$ and it is acted as driving force on vortices by the sliding pinning potential. In other words, the 45° direction for $+I_a$ is a much easier direction than −135° for $-I_a$. As a consequence, the vortices always move along sliding directions but 45° is a much easier direction (see panels 1, 6 on the right of Fig. 2), which leads to a positive rectified voltage V_{dc}^x along x direction. Definitely, one can also observe a positive rectified voltage V_{dc}^y along y direction due to the horizontal component of the vortex motion.

With increasing ac current, a negative rectified voltage V_{dc}^x is observed in region Ⅱ. In this case, vortex velocity induced by Lorentz force is faster than sliding potential v_p and the sliding potential acted as pinning force. The magnitude of pinning effect depends on their relative velocity. The relative velocity between vortices and sliding potential for $+I_a$ is smaller than that for $-I_a$. Thus the pinning effect for $+I_a$ is larger than that for $-I_a$. This implies that −135° for $-I_a$ is a much easier direction now, which leads to a smaller resistance force on vortices (see panels 2, 7 on the right of Fig. 2 and the second panel in Fig. 2(e)). The similar mechanism for this reversal vortex rectification has been proposed.[22,23]

With further increase of ac current, in region Ⅲ, one can observe a positive rectified voltage V_{dc}^x again. In this case, as shown in the third panel of Fig. 2(e), the much easier direction of sliding channels can still attract vortices moving along −135° and the Lorentz force for $-I_a$ is still unable to drive vortices out of the channel (panels 8 and 9). However, the sliding channels with 45° cannot confine vortices anymore and the Lorentz force is strong enough to drive the vortices out of the sliding channels. Thus a partial vertical vortex motion can be observed along $+y$ direction in the case of $+I_a$ as shown in panels 3 and 4. The direct vertical vortex motion can contribute more to the voltage V^x for $+I_a$. This leads to a positive rectified voltage V_{dc}^x. Finally, a negative rectified voltage V_{dc}^x is observed in region Ⅳ with further increasing ac current. In this case, the current is very large and the Lorentz force is strong to drive the vortices out of sliding channel. Panels 5 and 10 show that there are two vortex jumps from a sliding channel to another in each vortex route for both $+I_a$ and $-I_a$. As such, the effects of vertical vortex motion on the voltage V^x for $+I_a$ and $-I_a$ are nearly same and the negative rectified voltage should result from the different vortex velocities in sliding channels for $+I_a$ and $-I_a$.

Then we discuss the developments of transverse voltages (so-called Hall voltage) as a function of ac amplitudes shown in Figs. 2(b) and 2(d). However, different from the longitudinal rectified voltage, the rectified transverse voltage V_{dc}^y has only one sign reversal of ratchet effect as shown in Fig. 2(b). Interestingly, the Hall voltages V^y is not a monotonic function of ac current amplitude from Fig. 2(d). It should be noted that when vertical vortex routes along $+y$ increase rapidly for $+I_a$ at $0.165 j_0 W \le I_{ac} < 0.19 j_0 W$, one can observe a decrease of V^y with increasing current as shown in points 3, 4 of Fig. 2(d). As ac current increases to $0.18 j_0 W$, V^y for $-I_a$ reaches the maximum and V^y for $+I_a$ has a local minimum. Consequently, the largest rectified voltage V_{dc}^y appears at $I_{ac} = 0.18 j_0 W$. With increasing ac current, the vortex motion also has vertical component for $-I_a$. This results in nearly the same voltage V^y for $-I_a$ and $+I_a$.

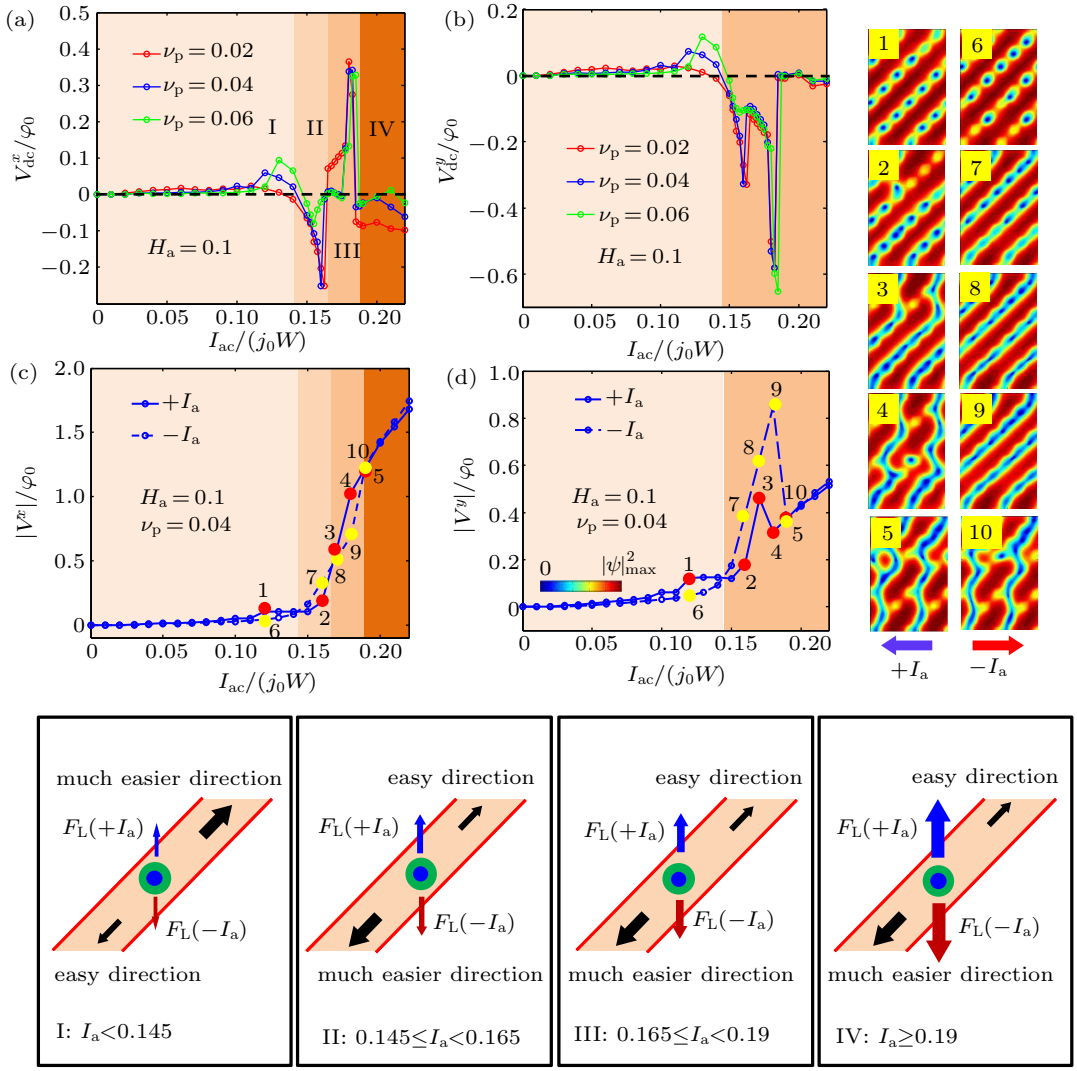


Fig. 2. The measured dc voltages V_{dc}^x (a) and V_{dc}^y (b) versus ac current amplitude I_{ac} at magnetic field $H_a = 0.1$ for several dynamic pinning velocities ν_p, respectively (multimedia view). The absolute values of longitudinal voltage V^x (c) and Hall voltage V^y (d) versus positive and negative current for $\nu_p = 0.04$. Panels 1–10 show the snapshots of Cooper-pair density for positive/negative current values in the I–V curves. The blue and red arrows indicate the directions of applied current for $+I_a$ and $-I_a$, respectively. (e) Schematic view of vortex rectification mechanisms for the four regions with increasing ac current amplitudes. The sliding potential can restrict vortices moving in the channel (the shaded area). The black thick and thin arrows (45° and −135° directions) indicate the much easier or easy direction for vortex motion compared with other directions. The blue and red arrows indicate the Lorentz force acting on vortices for $+I_a$ and $-I_a$, respectively. With increasing currents, the arrows becomes bigger, implying the larger Lorentz force.

Figures 3(a) and 3(b) show the variations of longitudinal and transverse ratchet effect versus dynamic pinning velocity for different ac currents at $H_a = 0.1$. The rectified voltages V_{dc}^x and V_{dc}^y are both monotonic functions of velocity ν_p. Surprisingly, for $I_{ac} = 0.18\, j_0W$ the variations of V_{dc}^x and V_{dc}^y versus ν_p become extraordinary. The dc voltages first increase rapidly, then keeps flat for $\nu_p \leq 0.1$, after that, the ratchet effects disappear. This means that the rectification becomes strongest at $I_{ac} = 0.18\, j_0W$ for a wide range of dynamic pinning velocity (see also the red region in $I_{ac} \sim \nu_p$ phase diagram). Another interesting feature is that the sign of V_{dc}^x is opposite to that of V_{dc}^y but at other ac amplitudes V_{dc}^x and V_{dc}^y keep the same sign. This is ascribed to the fact that at larger currents, vortices bend to move along the direction of Lorentz force for $+I_a$ and $\nu_p \leq 0.1$ (panels 1–3). While the vortices move along tilted straight lines for $-I_a$. Therefore, the voltage V^x for $+I_a$ is larger than that for $-I_a$ but V^y for $+I_a$ is smaller than that for $-I_a$. However, for much larger ν_p, the winding vortices translate into vortex chains for $+I_a$ (panel 4). The effect of dynamic pinning potential on vortex motion is almost the same for $+I_a$ and $-I_a$ under this condition. This leads to nearly no ratchet effect.

Figures 4(a) and 4(b) illustrate the developments of the rectified dc voltage V_{dc}^x and V_{dc}^y versus ac current amplitude at $H_a = 0.2$, respectively. By contrast to the case of $H_a = 0.1$, the first peak of rectified voltage occurs earlier for the smaller dynamic pinning velocity. There is only one reversal for longitudinal ratchet effect but four reversals for transverse ratchet effect. The crossed phase slip lines both exist for $+I_a$ and $-I_a$. However, the voltage V^x is monotonic as a function of

I_{ac}, which for $-I_a$ is always larger than that for $+I_a$ in the current $I_{ac} > 0.09 j_0 W$ as shown in the $V(t)$ curve of Fig. 4(c). Hall voltage V^y oscillates with I_{ac}, and Hall voltage for $-I_a$ is sometimes larger and sometimes less than that for $+I_a$. The out of sync jump induced by phase slip lines as shown in Fig. 4(d) is responsible for the multiple reversals of ratchet effect.

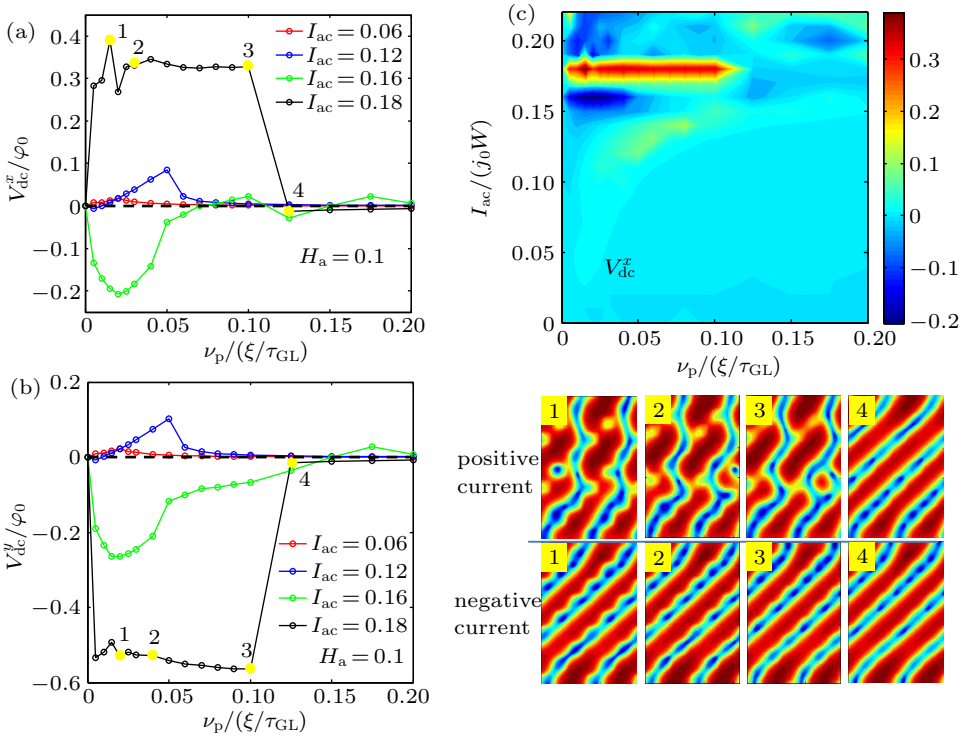


Fig. 3. The dc voltages V_{dc}^x (a) and V_{dc}^y (b) versus dynamic pinning velocity ν_p (multimedia view). Panels 1–8 show the snapshots of Cooper-pair density for different dynamic pinning velocities in the V_{dc}–ν_p curves. (c) The I_{ac}–ν_p phase diagram of the rectified voltage V_{dc}^x at magnetic field $H_a = 0.1$.

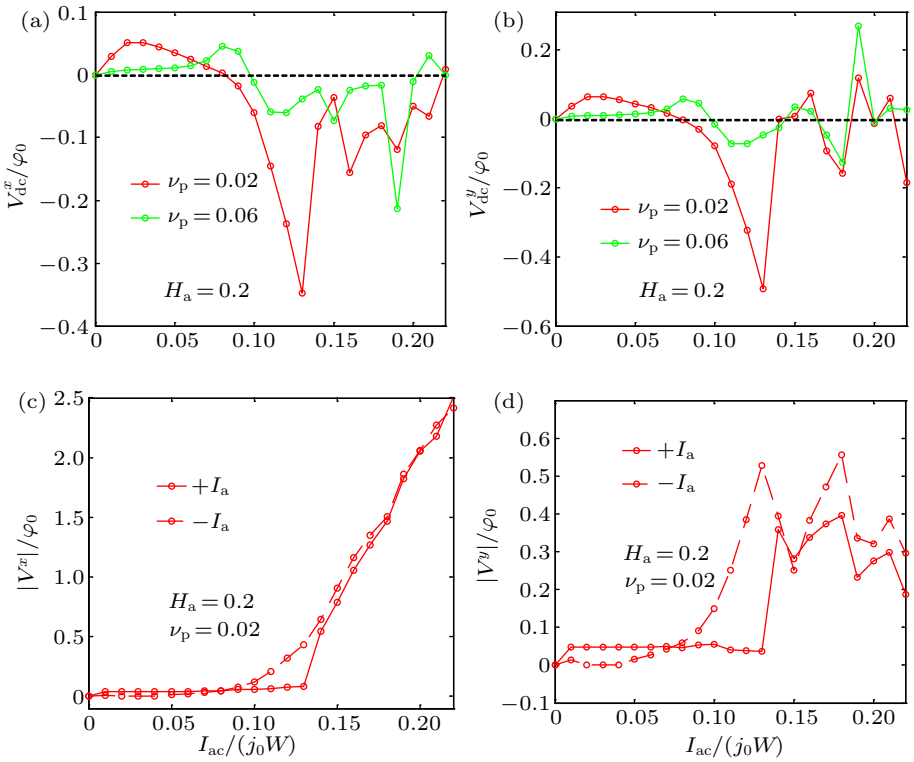


Fig. 4. The measured dc voltages V_{dc}^x (a) and V_{dc}^y (b) as a function of ac current amplitude I_{ac} at magnetic field $H_a = 0.1$ for several dynamic pinning velocities, respectively. The absolute values of longitudinal voltage V^x (c) and Hall voltage V^y (d) versus positive and negative current for $\nu_p = 0.02$, respectively.

Figure 5 shows the same developments of rectified dc voltage versus dynamic pinning velocity as Fig. 3 but at $H_a = 0.2$. It is obvious that the rectified voltage exhibits no reversible ratchet effect at smaller currents. However, different from Fig. 3, at the intermediate ac amplitude $I_{ac} = 0.1$, the reversible ratchet effect versus ν_p is observed. This transition is caused by the relative velocity of vortex motion to sliding pinning. At smaller velocities, the dynamic pinning sites impede the vortex motion for $+I_a$ while the vortices move preferentially against the direction of dynamic pinning potential for $-I_a$. This leads to the negative rectified voltage at smaller ν_p. However, on the contrary, vortices for larger ν_p move more quickly along the direction of dynamic pinning sites for $+I_a$ than that for $-I_a$. As a consequence, positive rectified voltage appears at larger ν_p. As ac current increases to $I_{ac} = 0.19 j_0 W$, the rectification becomes strongest in the wide range of $0.03 \leq \nu_p \leq 0.1$.

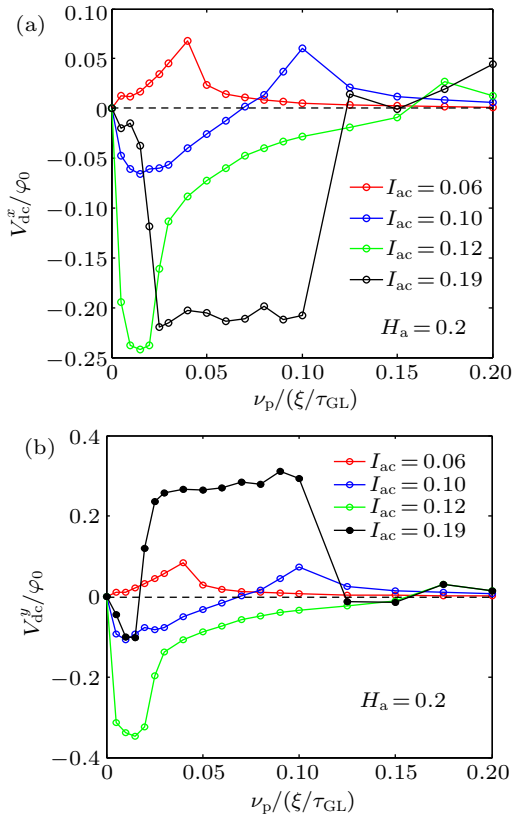


Fig. 5. The variations of V_{dc}^x (a) and V_{dc}^y (b) versus ν_p at $H_a = 0.2$, respectively.

4. Conclusion

In summary, the vortex dynamics and rectifications of a superconducting strip by tilted dynamic pinning potential is investigated using the time-dependent Ginzburg–Landau equations. Due to the inclination angle of Lorentz force with respect to sliding potential direction, the sliding potentials confine vortices moving in the tilted channels, but the Lorentz forces try to drive vortices out of the channels. This leads to a complicated background for vortex dynamics owing to the competition between Lorentz force and sliding potential. Depending on ac amplitude and sliding potential velocity, multiple reversal of transverse and longitudinal ratchet effect can be observed for different magnetic fields. The reversal mechanisms of vortex rectifications are illustrated by the change of easier direction for vortex motion. The consideration of easier direction is not only along the tilted channels but also vertical Lorentz force. The oscillation of Hall voltage versus current value denotes a distinct characteristic from the traditional current-voltage curve. This is due to the increased vertical vortex routes with increasing current amplitude. Moreover, when the applied current is large enough in which the Lorentz force dominates, the ratchet effect reaches strongest within a wide range of velocity ν_p. The approach could also be useful for the manipulation of vortices in the iron-chalcogenides and the Majorana zero modes in their cores[44–47] for topological quantum computing. This technique could be used to make something like a quantum computing punch card. Such a version of this idea has ever been proposed for a single trap.[48] The ability to manipulate a large array of traps could mean that this approach could be scaled up.

Supplementary figures

See the supplementary movies (M1, M2, M3, M4, M5) for the ratchet effect at $H_a = 0.1$ for different ac current amplitudes as shown in Fig. 2.

References

[1] Wördenweber R and Dymashevski P 2004 *Phys. Rev. B* **69** 184504
[2] Wördenweber R, Sankarraj J S K, Dymashevski P and Hollmann E 2006 *Physica C* **434** 101
[3] Auslaender O M, Luan L, Straver E W J, Hoffman J E, Koshnick N C, Zeldov E, Bonn D A, Liang R, Hardy W N and Moler K A 2009 *Nat. Phys.* **5** 35
[4] Ma X. Y, Reichhardt C J O and Reichhardt C 2018 *Phys. Rev. B* **97** 214521
[5] Lee C S, Jankó B, Deré nyi I and Barabási A L 1999 *Nature* **400** 337
[6] Villegas J E, Savel'ev S, Nori F, Gonzalez E M, Anguita J V, Garcia R and Vicent J L 2003 *Science* **302** 1188
[7] Souza Silva C C, Van de Vondel J, Morelle M and Moshchalkov V V 2006 *Nature* **440** 651
[8] Souza Silva C C, Silhanek A V, van de Vondel J, Gillijns W, Metlushko V, Ilic B and Moshchalkov V V 2007 *Phys. Rev. Lett.* **98** 117005
[9] Zhu B Y, Marchesoni F and Nori F 2004 *Phys. Rev. Lett.* **92** 180602
[10] Gillijns W, Silhanek A V, Moshchalkov V V, Reichhardt C J O and Reichhardt C 2007 *Phys. Rev. Lett.* **99** 247002
[11] Van de Vondel J, Gladilin V N, Silhanek A V, Gillijns W, Tempere J and Moshchalkov V V 2011 *Phys. Rev. Lett.* **106** 137003
[12] Lu Q M, Olson Reichhardt C J and Reichhardt C 2007 *Phys. Rev. B* **75** 054502
[13] Berdiyorov G R, Milošević M V, Covaci L and Peeters F M 2011 *Phys. Rev. Lett.* **107** 177008
[14] Reichhardt C, Ray D and Olson Reichhardt C J 2015 *Phys. Rev. B* **91** 184502
[15] Adami O A, Cerbu D, Cabosart D, Motta M, Cuppens J, OrtizWA, Moshchalkov V V, Hackens B, Delamare R, Van de Vondel J and Silhanek A V 2013 *Appl. Phys. Lett.* **102** 052603
[16] Ji J D, Yuan J, He G, Jin B H, Zhu B Y, Kong X D, Jia X Q, Kang L, Jin K and Wu P H 2016 *Appl. Phys. Lett.* **109** 242601

[17] Cerbu D, Gladilin V N, Cuppens J, Fritzsche J, Tempere J, Devreese J T, Moshchalkov V V, Silhanek A V and Van de Vondel J 2013 *New J. Phys.* **15** 063022

[18] Cole D, Bending S, Savel'ev S, Grigorenko A, Tamegai T and Nori F 2006 *Nat. Mater.* **5** 305

[19] Wang Y L, Ma X Y, Xu J, Xiao Z L, Snezhko A, Divan R, Ocola L.E, Pearson J E, Janko B and Kwok W K 2018 *Nat. Nanotech.* **13** 560

[20] Jelić Ž L, Milošević M V, Van de Vondel J and Silhanek A V 2015 *Sci. Rep.* **5** 14604

[21] Jelić Ž L, Milošević M V and Silhanek A V 2016 *Sci. Rep.* **6** 35687

[22] He A, Xue C and Zhou Y H 2019 *Appl. Phys. Lett.* **115** 032602

[23] Cun Xue, He A, Milošević M V, Silhanek A V and Zhou Y -H 2019 *New J. Phys.* **21** 113044

[24] Giaever I 1965 *Phys. Rev. Lett.* **15** 825

[25] Giaever I 1966 *Phys. Rev. Lett.* **16** 460

[26] Solomon P R 1966 *Phys. Rev. Lett.* **16** 50

[27] Ekin J W, Serin B and Clem J R 1974 *Phys. Rev. B* **9** 912

[28] Aladyshkin A Y, Silhanek A V, Gillijns W and Moshchalkov V V 2009 *Supercond. Sci. Technol.* **22** 053001

[29] Kramer R B G, Silhanek A V, Gillijns W and Moshchalkov V V 2011 *Phys. Rev. X* **1** 021004

[30] Rodrigo P J, Eriksen R L, Daria V R and Glückstad J 2002 *Opt. Express* **10** 1550

[31] Brunner M and Bechinger C 2002 *Phys. Rev. Lett.* **88** 248302

[32] Grier D G 2003 *Nature* **424** 810

[33] Lee S H, Ladavac K, Polin M and Grier D G 2005 *Phys. Rev. Lett.* **94** 110601

[34] Libál A, Reichhardt C, Jankó B and Olson Reichhardt C J 2006 *Phys. Rev. Lett.* **96** 188301

[35] Bumby C W, Jiang Z, Storey J G, Pantoja A E and Badcock R A 2016 *Appl. Phys. Lett.* **108** 122601

[36] Kramer L and Watts-Tobin R J 1978 *Phys. Rev. Lett.* **40** 1041

[37] Berdiyorov G, Harrabi K, Oktasendra F, Gasmi K, Mansour A I, Maneval J P and Peeters F M 2014 *Phys. Rev. B* **90** 054506

[38] Watts-Tobin R J, Krähenbühl Y and Kramer L 1981 *J. Low Temp. Phys.* **42** 459

[39] Berdiyorov G R, Milošević M V and Peeters F M 2009 *Phys. Rev. B* **79** 184506

[40] Berdiyorov G R, Milošević M V, Latimer M L, Xiao Z L, Kwok W K and Peeters F M 2012 *Phys. Rev. Lett.* **109** 057004

[41] Lombardo J, Jelić Ž L, Baumans X D A, Scheerder J E, Nacenta J P, Moshchalkov V V, Van de Vondel J, Kramer R B G, Milošević M V and Silhanek A V 2018 *Nanoscale* **10** 1987

[42] Adami O A, Jelić Ž L, Xue C, Abdel-Hafiez M, Hackens B, Moshchalkov V V, Milošević M V, Van de Vondel J and Silhanek A V 2015 *Phys. Rev. B* **92** 134506

[43] Kramer R B G, Ataklti G W, Moshchalkov V V and Silhanek A V 2010 *Phys. Rev. B* **81** 144508

[44] Beenakker C W J, Baireuther P, Herasymenko Y, Adagideli I, Lin Wang and Akhmerov A R 2019 *Phys. Rev. Lett.* **122** 146803

[45] Wang D, *et al.* 2018 *Science* **362** 333

[46] Kong L, *et al.* 2019 *Nat. Phys.* **15** 1181

[47] Kong L and Ding H 2020 *Acta Phys. Sin.* **69** 110301 (in Chinese)

[48] Ma X, Reichhardt C J O and Reichhardt C 2020 *Phys. Rev. B* **101** 024514